Transactions on Biomedicine and Health vol 3, © 1996 WIT Press, www.witpress.com, ISSN 1743-3525

Visualization of computer-generated arterial model trees

F. Neumann, M. Neumann, R. Karch, W. Schreiner
Institute of Experimental Physics, Dept. of Surgery & Dept. of Medical Computer Sciences, University of Vienna, A-1090 Wien, Austria

Abstract

By our method of "constrained constructive optimization" we generate, on the computer, highly realistic models of coronary arterial trees comprising on the order of 10^4 individual segments. To characterize these complex structures not only by statistical means, application-specific algorithms and computer programs have been developed to visually display their particular branching pattern. The entire tree is rendered in a realistic, three-dimensional manner, similar to the appearance of corrosion casts of real arterial trees. Additionally, various physical and physiological properties can be visualized by appropriate color-coding.

1 Introduction

In contrast to compartmental and multi-layer models of the coronary circulation, model trees consisting of individual segments can be generated by the method of "constrained constructive optimization " (CCO, Schreiner[1]). Arterial trees are simulated in full detail from the feeding artery ($r \approx 1.5\,\mathrm{mm}$) down to terminal segments with radii of approximately $50\,\mu$. When compared to stochastic models, where vessel segments are also considered in detail, CCO trees exhibit a "realistic" geometrical arrangement of vessels comparable to corrosion casts of real arterial trees. These computer-generated tree structures form the basis of hemodynamic simulations, in which the dependency of coronary blood flow on the structure of the tree, the properties of the vessels, as well as on various external parameters is investigated.

The structure of these complex model trees can be theoretically de-

scribed and analyzed by statistical means. But only a visual representation of the entire vessel tree is able to reveal its global shape and geometry. Although our vascular model trees, being essentially an assembly of simple geometrical objects, could, in principle, be visualized by means of a ray tracer or a graphics package capable of CSG (constructive solid geometry), we have nevertheless found it necessary to write a set of application-specific visualization programs in a conventional programming language. The specific programs are more flexible and efficient, and independent of the computer hardware and operating system. A quasi-realistic representation of vessel trees with arbitrary surface shading and lighting is obtained.

2 CCO tree structures

In CCO model trees, anatomical and physiological principles are taken into account by the specific choice of boundary conditions, constraints, and target function for geometrical and structural optimization (Schreiner *et al.*[2]). Presently, the trees are generated within an arbitrary (usually circular) two-dimensional area representing a piece of tissue to be perfused. (The generalization to genuine three-dimensional structures is underway.) The terminal segments of these binary trees are required to be uniformly distributed within this area to perfuse it as homogeneously as possible. The resolution of the tree is given by the number of terminal segments N_{term}. For dichotomously branching trees, the total number of segments is always given by $N_{\text{tot}} = 2N_{\text{term}} - 1$, regardless of the particular structure of the tree.

The tree is grown by successively adding terminal segments at randomly chosen perfusion sites and generating new bifurcations. In accordance with morphometric measurements on corrosion casts of real arterial trees, the radii of parent and daughter segments at each bifurcation obey a power law

$$r_{\text{parent}}^{\gamma} = r_{\text{left}}^{\gamma} + r_{\text{right}}^{\gamma}\,, \tag{1}$$

with typical values of γ falling in the range between 2.5 and 3.

In order to perfuse a circular area of radius $r_{\text{perf}} = 5\,\text{cm}$ under "physiological" conditions, perfusion pressure, terminal pressure, and total perfusion flow are set to $p_{\text{perf}} = 100\,\text{mm Hg}$, $p_{\text{term}} = 60\,\text{mm Hg}$, and $Q_{\text{perf}} = 500\,\text{ml/min}$, respectively, and kept constant in all simulations. After adding a new bifurcation, segment radii are rescaled according to Poiseuille's law for laminar flow resistance so that all terminal segments deliver equal flows ($Q_{\text{term}} = Q_{\text{perf}}/N_{\text{term}}$) at equal pressures ($p_{\text{term}}$).

Additionally, the geometrical location of each bifurcation is optimized by minimizing a cost (or target) function which is defined in terms of the functional structure of the tree. Suitable cost functions for structural optimization may be derived from global properties of the vascular tree and

Transactions on Biomedicine and Health vol 3, © 1996 WIT Press, www.witpress.com, ISSN 1743-3525

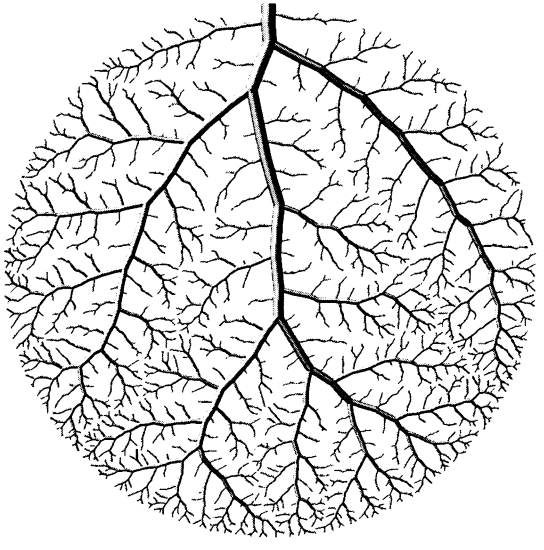

Figure 1: CCO-generated arterial model tree with parameters $\gamma = 3$ [Eq. (1)] and $\lambda = 2$ [Eq. (2)]. Segments with $r < 100\,\mu$ have been omitted ("pruned") for reasons of clarity. Visualization was performed using geometrical primitives (cf. Sec. 3.1).

were chosen to be of the general form

$$T = \sum_{i=1}^{N_{\text{tot}}} \ell_i \, r_i^{\lambda} \rightarrow \min , \tag{2}$$

where ℓ_i and r_i are length and radius of segment i. The exponent may take on every real value $\lambda \geq 0$. Setting λ equal to 0, 1, or 2 is equivalent to minimizing total vessel length, surface or intravasal volume, respectively (cf. Figs. 1 and 4). Thus, not only the geometrical location of a single bifurcation, but also the global topological structure of the tree is optimized according to the target function.

3 Visualization of CCO trees

In order to evaluate and characterize the properties of CCO trees not only numerically or statistically, it was felt desirable to be able to visualize the generated structures in a way comparable to corrosion casts of real arterial trees. Parameter variations in CCO yield a variety of geometrical structures which more or less resemble such corrosion casts. Usually even a superficial

inspection of a visualization already permits a first assessment of the degree of similarity between the generated structures and real arterial trees. For instance, comparing Figs. 1 and 4 clearly shows that the geometry of CCO trees crucially depends on the parameter λ of the target function. Moreover, physical and physiological properties of CCO trees, such as flow velocity or wall shear stress and their spatial or temporal variation, can be visualized by color coding of individual segments. On the other hand, color coding can also be used to illustrate rather abstract notions, such as, for instance, classifications of vessel segments according to topological concepts.

As described in the previous section, computer generated CCO trees consist of a particular arrangement of cylindrical tubes. One would therefore think that visualizing the whole structure of the tree by means of a ray tracer or even a simple rendering program capable of CSG should be straightforward. Such programs are able to visualize primitive geometrical objects (cylinders, cones, spheres, etc.) as well as their unions, intersections and differences (Foley[4], Watt[5], Wolff[6]). In our special case, however, the practicability of such general packages is very limited for two reasons. First, the large number [presently $O(10^4)$] of segments to be rendered would be highly demanding in terms of computer time; second, because of the lack of a geometrical representation of bifurcations: In the CCO model, the geometry of the bifurcation is completely ignored; to visualize the resulting structures, however, some assumption has to be made as to how a parent segment is joined to its daughter segments. We defined a simple geometrical *ad-hoc* construction as described in the following section, which yields optically satisfying results for anatomically "realistic" arterial trees (cf. Fig. 1). Since the objects resulting from this geometrical construction cannot be easily represented by the primitives of a general rendering package, specific computer programs were written in a conventional programming language.

Visualizing a vascular tree as an assembly of simple geometrical objects is simple and very efficient, but unsatisfactory results are sometimes obtained for "pathological" structures, such as short segments bifurcating at obtuse angles or turning backwards (see Fig. 4, upper tree). Therefore, we have developed an alternative algorithm which is conceptually based on isosurfaces, and in which bifurcations appear "automatically", without explicit geometrical definition of their shape. This method has provided optically very convincing results in all cases investigated so far. Again, instead of using a general graphics package, the algorithm had to be implemented as a conventional computer program, which is rather CPU-intensive. However, it was the only reasonable approach that allowed us to obtain the high resolution necessary for visualizing the delicate structure of our CCO-generated arterial trees.

3.1 Object-based rendering

Our first attempt was an object-based approach, i.e. the CCO tree was decomposed into simple geometrical elements, namely cylinders and (truncated) cone-like objects, representing the vessel segments and their connections at bifurcations (see below). The surfaces of all elements were sampled with sufficiently high resolution, shaded according to the Phong reflection model, and projected onto the image plane. A Z-buffer algorithm was used to account for visibilities: for each pixel of the frame buffer a depth value is stored corresponding to the nearest object point rendered so far; a new value is stored only if a point closer to the viewer is encountered (Foley[4], Watt[5], Wolff[6]).

Sampling was performed by mapping a sufficiently fine cartesian grid onto the surface of the objects. This was easily achieved both for cylindrical and cone-like objects, as the surface of the truncated "cones" forming the bifurcation was simply defined to be the shape obtained by joining corresponding points on the perimeter of the parent and daughter segments by straight lines. To avoid overlaps, the cylindrical elements were truncated just enough to be smoothly connected by these cone-like objects (see Fig. 2).

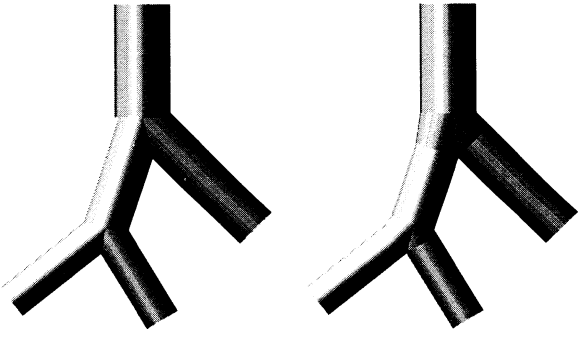

Figure 2: Representation of isolated bifurcations. *Left*: overlapping cylinders, corresponding literally to the CCO model; *right*: parent and daughter segments are shortened and joined by truncated cone-like objects.

Images of nearly photo-realistic quality were obtained when shading was performed by means of the Phong model, which accounts in a simple way for diffuse and specular reflection. The intensity emitted from a surface point of the object is (for any of the three color components $c = \mathrm{R}, \mathrm{G}, \mathrm{B}$) given by

$$I_c = I_{c,a} k_{c,a} + \sum_i I_{c,p_i} (k_{c,d} \cos \alpha_i + k_s \cos^n \beta_i) \,, \qquad (3)$$

where k_a, k_d and k_s are the coefficients of reflection for ambient light, diffuse and specular reflection, respectively; I_a is the intensity of ambient light and I_{p_i} the intensity of the i-th light source. α_i is the angle between the surface normal and the direction to light source i, β_i is the angle between the mirror-like reflected light ray from light source i and the direction to the observer, and n is a parameter controlling the spatial extent of specular highlights (Foley[4], Watt[5], Wolff[6]).

3.2 Image-based rendering (isosurfaces)

Object-based rendering as described in the previous section has proved to be reasonably efficient, even at high resolution and for arterial trees consisting of several thousand segments. In most cases the visualizations do in fact look like photographical images of corrosion casts of real arterial trees. However, CCO trees generated under obviously unrealistic conditions may exhibit "pathological" structures. For instance, putting $\lambda = 0$ in the target function, Eq. (2), yields long meandering structures consisting of many short segments which frequently turn backwards and give off small side branches under obtuse bifurcation angles. Clearly, a purely geometrical construction is bound to break down in these cases (cf. Fig. 4, top). In order to visualize also these structures in a plausible manner, we used an image-based direct volume rendering (DVR) technique, where the entire vascular tree is represented by a single isosurface of a suitable "potential" (Watt[5], Wolff[6]). In this way bifurcations formed by segments of arbitrary dimensions and branching angles are rendered automatically, without the need to explicitly define their shape in geometrical terms.

Our approach can be most easily explained with the help of concepts borrowed from electrostatics (Jackson[7]). Starting with a single segment i of an arterial tree, we assume that a uniform (one-dimensional) electrical charge density, $\tau(s) \equiv \tau$, is distributed along its axis of symmetry. In this case the electrostatic potential at position $\mathbf{x}$ due to the line charge on segment i is given by

$$\Phi_i(\mathbf{x}) = \int_0^{\ell_i} ds\, \varphi_i[\mathbf{x} - \mathbf{x}_i(s)]\tau(s)\,, \tag{4}$$

where ℓ_i is the total length of segment i, s is the arclength, $\mathbf{x}_i(s)$ is the parameterization of the symmetry axis, and $\varphi_i(\mathbf{x})$ is a function describing the interaction between two unit charges separated by a distance $\mathbf{x}$. In electrostatics, we have $\varphi(\mathbf{x}) = 1/|\mathbf{x}|$, but here we may use any function which decays sufficiently fast at infinity. In particular, we may assume φ_i to be different for each segment; this will be utilized to assign segments their individual radii. For reasons of symmetry, the equipotential surface (i.e. the isosurface where Φ_i takes on a particular threshold value C) for a single segment of infinite length is a cylinder; for a segment of finite length, a cigar-shaped object is obtained.

Continuing the electrostatic analogy, the potential generated by a complete CCO tree is simply the linear superposition of the potentials produced by its individual segments

$$\Phi(\mathbf{x}) = \sum_i \Phi_i(\mathbf{x}) = \sum_i \int_0^{\ell_i} ds\, \varphi_i[\mathbf{x} - \mathbf{x}_i(s)]\tau(s)\,, \tag{5}$$

and the visualization surface of the tree is the set of all points for which $\Phi(\mathbf{x}) = C$. For reasons of convenience, we have used Gaussians for the φ_i's

$$\varphi_i(\mathbf{x}) = \frac{1}{\sqrt{2\pi}(r_i/2)} e^{-\mathbf{x}^2/2(r_i/2)^2}\,, \tag{6}$$

since the integrals in Eq. (5) can then be expressed analytically and the calculation of $\Phi(\mathbf{x})$ reduces to a simple sum.

Due to the rapid decay of Gaussians, only a few segments will contribute to the value of $\Phi(\mathbf{x})$ at any given point, provided that the parameters are chosen approximately. As can be seen from Eq. (5), the width of the Gaussians was linked to the segment radii r_i, so that φ_i is in fact different for each segment. To ensure that long segments will be rendered as cylindrical objects with apparent radius r_i, a threshold value consistent with Eq. (5) has to be used; in our case it is given by $C/\tau = e^{-2} \approx 0.13533$. This particular choice of widths and threshold value produced excellent results, but a different parameterization of the Gaussians, or even using a different functional form could yield similarly satisfying results.

Isosurfaces are most efficiently visualized by means of one of the polygon-based rendering procedures included in many graphics packages (Watt[5], Wolff[6]). However, this requires prior calculation of the "potential" on a sufficiently fine three-dimensional grid. Since this is not feasible given the high resolution necessary to display our tree structures, we have implemented a direct volume rendering technique which is a simple variant of the ray casting method (Watt[5]). A ray is fired through each pixel of the image plane, and its first intersection with the isosurface is determined. At that location, background lighting, diffuse and specular reflection are calculated exactly in the way described in the previous section, except that the surface normal is now obtained from the gradient of the potential, $\mathbf{n} = \nabla\Phi(\mathbf{x})/|\nabla\Phi(\mathbf{x})|$, and the pixel value is set accordingly. Since this algorithm is extremely CPU-intensive [$\Phi(\mathbf{x})$ has to be sampled frequently enough along the ray to find the first intersection], segments are pre-selected with the help of bounding volumes. Thus, for each pixel only those segments will actually be considered in Eq. (5), which may be expected to yield a non-zero contribution.

Figure 3 shows by means of a simple example that the isosurface method, which is based on fictitious potentials, is vastly superior compared to the geometrical approach of the previous section: acute as well as obtuse-angled

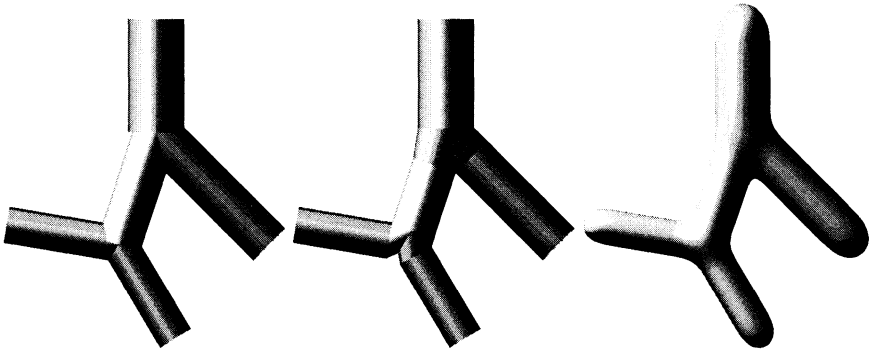

Figure 3: Visualization of isolated bifurcations. *Left*: overlapping cylinders; *center*: geometrical rendering of cylinders and joining cone-like objects; *right*: isosurface method, showing convincing representation of all types of branching angles.

bifurcations are now rendered in an absolutely convincing manner. In particular, the isosurface algorithm automatically results in a very plausible representation of the bifurcation as such, which could not be readily defined in geometrical terms. This comes, of course, at a price: calculating and rendering of isosurfaces is also vastly more time-consuming than geometrical rendering!

Finally, Fig. 4 shows a full CCO tree which was optimized with respect to the minimum sum of segment lengths [i.e., $\lambda = 0$ in Eq. (2)]. Physiologically, the resulting structure may be considered as "pathological"; however, it is obvious that even in cases like this the isosurface method yields a perfectly convincing visual representation.

Presently, the isosurface algorithm is being used to generate three-dimensional representations of two-dimensional tree structures. However, the computer programs in their present form are immediately applicable to visualizations of future three-dimensional generalizations of CCO trees. Moreover, the algorithm is not restricted to computer generated trees, but can also be used to visualize experimental structures, if the precise spatial dimensions are available from the measurements.

Lastly, a brief word on hardcopy output capabilities. As usual, during the early stages of this work we had several parallel versions of each program, each specialized for a specific type of output device (screen, paper, digital film printer, video...) and slowly drifting away from its companions. Consequently, we have now restricted all output to a single intermediate format, and the conversion to a format appropriate for a specific

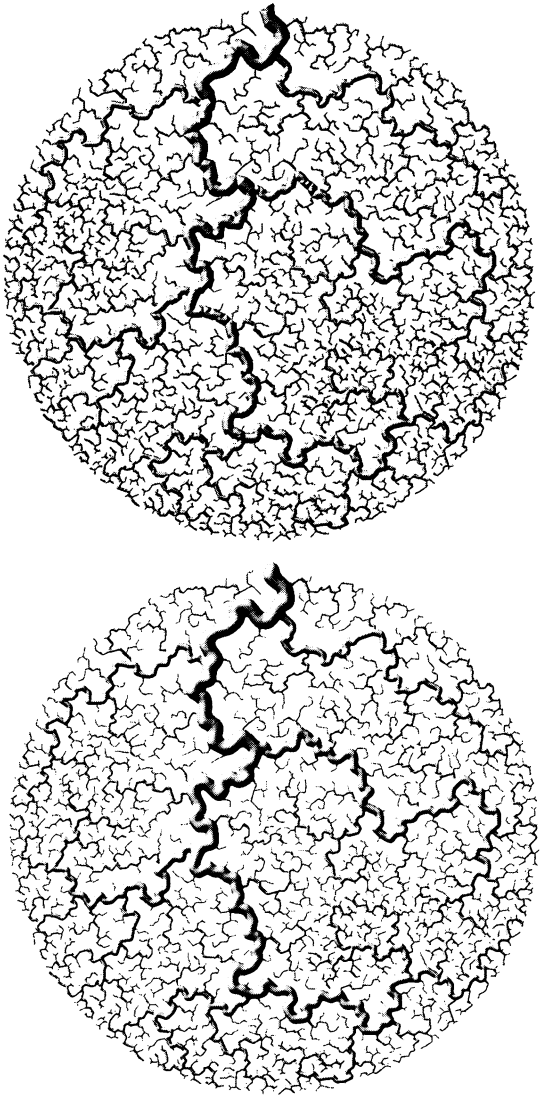

Figure 4: CCO-generated arterial model tree with parameters $\gamma = 3$ and $\lambda = 0$ in Eqs. (1) and (2). As in Fig. 1, segments with $r < 100\,\mu$ have been pruned for clarity. Visualization was performed using object-based geometrical rendering (*top*) as well as image-based direct volume rendering (isosurface, *bottom*).

device is handled by a separate program. The intermediate format chosen by us is ppm (portable pixmap), which is straightforward to implement, and for which a large number of converters is available in the public domain "pbmplus" package (Murray & van Ryper[8]). The ppm format can also be processed by many other graphics programs in the public domain as well as by commercial packages.

Key words

constrained constructive optimization
vascular trees
volume rendering
ray casting
isosurfaces

References

1. Schreiner, W. Computer generation of complex arterial tree models, *Journal of Biomedical Engineering*, 1993, **15**, 148–150.

2. Schreiner, W. & Buxbaum, P. Computer-optimization of vascular trees, *IEEE Transactions of Biomedical Engineering*, 1993, **40**, 482–491.

3. Schreiner, W., Neumann, F., Neumann, M., End, A., Rödler, S.M. & Aharinejad, S. The influence of optimization target selection on the structure of arterial tree models generated by constrained constructive optimization, *Journal of General Physiology*, 1995, **106**, 583–599.

4. Foley, J.D. & van Dam, A. *Fundamentals of Interactive Computer Graphics*, Addison-Wesley, Reading MA, 1982.

5. Watt, A. & Watt, M. *Advanced Animation and Rendering Techniques. Theory and Practice*, Addison-Wesley, Wokingham, 1992.

6. Wolff, R.S. & Yaeger, L. *Visualization of Natural Phenomena*, Springer-Verlag, New York, 1993.

7. Jackson, J.D. *Classical Electrodynamics*, 2nd edition, Wiley, New York, 1975.

8. Murray, J.D. & van Ryper, W. *Encyclopedia of Graphics File Formats*, O'Reilly and Associates, Sebastopol CA, 1994.